Autophagy-Sirtuin1(SIRT1) Modulated The Endothelial Progenitor Cells (EPCs) Proliferation and Migration Via wnt/β-Catenin/GSK3β Signaling Pathway and Alleviated The Coronary Atherosclerosis (CAS) in Mice

Yanwei Li
Tianjin First Central Hospital
Wei Cui
Jinzhou Inspection and Testing Cerfication Center of liaoning PROVINCE
Bing Song
The First Affiliated Hospital of Jinzhou Medical University
Xuying Ye
Tianjin First Central Hospital
Zhuqing Li
Nankai University
Chengzhi Lu (fdxl5656@126.com)
Tianjin First Central Hospital https://orcid.org/0000-0003-4105-2969

Routine Article

Keywords: SIRT1, EPCs, CAS wnt/β-catenin/GSK3β, autophagy

Posted Date: February 17th, 2021

DOI: https://doi.org/10.21203/rs.3.rs-203648/v1

Abstract

Background and purpose: SIRT1 exerted its link to CAS risk in humans and EPCs presented its reparative role in CAS. In this study, we explored the role of SIRT1 in CAS mice and also its modulation in EPCs.

Methods and materials: ApoE-/- mice were fed with high-fat and high-glucose food to establish the CAS animal model with the normally-raised C57BL/6 mice as a healthy control group. 5 ApoE mice were intravenously injected with SIRT1 activator, SRT 2104 and another 5 were injected with inhibitor Nicotinamide in tail. Weight changes were recorded per week. Blood samples were taken from posterior orbital venous plexus and detected by automatic biochemical analyzer for lipid concentrations. Coronary artery tissues were observed. HE staining displayed the pathological condition while Immunohistochemistry (IHC) evaluated the CD34+/VEGFR2+ relative density. In vitro, EPCs were isolated from bone marrow each group and then purified, cultured and verified using immunofluorescence staining (IFS). Thereafter, we examined the modulatory mechanism of SIRT1 in EPCs by RT-PCR, MTT, Western Blot (WB) and colony formation, scratch methods, connecting the wnt/β-catenin/GSK3β signaling pathway.

Results：SIRT1 activation negatively regulated the weight and TC, TG and LDL. SIRT1 activator alleviated the lesion area and decreased the CD34+/VEGFR2+ density which was higher in coronary artery tissues in CAS and SIRT1 inhibitor groups. In vitro, SIRT1 activator promoted the bone marrow-derived EPCs proliferation, migration and activated wnt/β-catenin/GSK3β signaling pathway while inhibited the autophagy biomarkers ATG1 and LC3II. Furthermore, inhibition of autophagy led to the upregulation of SIRT1 and increase in cell proliferation, migration and wnt/β-catenin/GSK3β activity. The suppression of the pathway in turn lowered SIRT1 expression in EPCs, attenuated the cell proliferation and migration and promoted autophagy.

Conclusion: Taken all the findings together, this research disclosed that SIRT1 activator might perform its protective role in CAS through autophagy inhibition via wnt/β-catenin/GSK3β signaling pathway in EPCs.

Introduction

Atherosclerosis features focal lesions of cholesterol, inflammation and fibrosis in arteries, initiated by dysfunction of endothelium[1]. Endothelial dysfunction facilitates further infiltration of lipids, inflammation, bringing endothelial monolayer injury and disturbing the endothelium homeostasis and meanwhile EPCs migrate from bone-marrow to the injured area to regenerate and repair the vascular endothelium[1]. Fundamentally, EPC levels influenced the coronary artery endothelial functions and neovascularization[2]. EPCs were noticed in the 1990s and due to its potential vasculogenesis and endothelial monolayer regeneration[3], were extensively investigated in coronary heart diseases thereafter both in clinical and experimental fields[4-7]. In CAS patients, decreased counts of EPCs are associated with the oxidised low-density lipoprotein (oxLDL) levels, a clinically significant index of CAS diagnosis[2]. A previous10-year study reported that the increased EPC number predicted better prognosis in CAS

patients[8]. Furthermore, EPC capture has been tried in stent technology and presented promising therapeutic values against restenosis yet remails to be further verified clinically [9, 10].

Currently, reduced levels of sirtuin 1(SIRT1) in serum was reported to be able to predict CAS plaques, which was significantly in accordance with the computed tomography angiography (CTA) in people with no major symptom[11].On the other hand, among CAS patients, the SIRT1 expression in peripheral blood is notably reduced compared to the healthy people in a HDL-dependent pattern[12]. In animals transgenic with SIRT1, cardioprotective trend and delayed aging were displayed as discovered[13]. In oxidative stress-stimulated EPCs in vitro, SIRT1 also showed its protective function by lowering the apoptosis rate of EPCs and promoting the NAD+ levels[14]. Furthermore, hypermethylation and histone modification of SIRT1 promoter could regulate the senescence and migration of EPCs[15]. A recent study revealed that autophagy activation could lead to vascular protection via inhibiting inflammation However, there are few studies that focused on autophagy in correlation with SIRT1 in EPCs. In human umbilical vein endothelial cells, treated with ox-LDL, SIRT1 expression was in positive association with the autophagy[16]. Previous works demonstrated a dual role of autophagy in EPCs□which is , insufficient autophagy in EPCs might induce endothelial dysfunction[17] while inhibition of autophagy via AMPK/mTOR pathway in EPCs could promote angiogenesis and wound healing[18]. We hypothesized that SIRT1 might be autophagy-modulated and play a part in EPCs proliferation, migration as well as in CAS alleviation. Therefore, we investigated the role and potential mechanism of SIRT1 in EPC modulation in vitro and also observed the correlation in vivo.

Methods

Animal study

All the experiments were performed strictly following the regulations of the First Affiliated Hospital of Jinzhou Medical University. 5 C57BL/6 mice and 15 ApoE-/- were from Beijing Experimental Animal Institute, Chinese Academy of Medical Sciences and raised for one-week adaptive feeding. Then, mice were fed with high-fat fodder daily which contained 10% lard, 1% cholesterol and 0.5% cholate in the CAS group while normal fodder was used to feed each C57BL/6 mouse in the blank group. After another 28 days, 5 ApoE-/- mice were intravenously injected with SIRT1 activator, SRT 2104 (100mg/kg) and another 5 ApoE-/- were injected with inhibitor Selisistat (10mg/kg) in tail once every two days, feeding as previously, which continued for 21 weeks (Shanghai Yuanye Biotech, China). Thereafter, mice were kept as previously treated till the 30W. Weight changes of each mouse were recorded on a weekly basis for each group and the lipid levels of TC, TG, HDL and LDL in the blood sampled from the postorbital venous plexus were detected using medical automatic biochemical analyzer (Hitachi, Tokyo, Japan) at Week 30 before sacrifice. Coronary artery was taken from each sacrificed animal, followed by HE staining and Immunohistochemistry methods.

HE staining

Coronary artery tissues were fixed using 4% formaldehyde and embedded in paraffin. Serial section was conducted with thickness of 5μm for each tissue slice and distance of 30μm from one slice to another utilizing the lab microtome. After dewaxing using xylene twice, each for 30 min, absolute ethyl alcohol (5min), 95% ethyl alcohol（5min）, 80% ethyl alcohol (5min) and double distilled water (5min) washed the sections. Hematoxylin and Eosin Staining Kit was purchased from Beyotime (Shanghai, China) and used strictly according to the producer's recommendations. The stained sections were dehydrated using pure ethyl alcohol and xylene was used to make the sections transparent. Finally, neutral gum was used to seal the sheet. The stained tissues were observed and pictured under microscope

IHC method

The glass slides containing 5-μm-thick tissue samples were put into the 40°C water bath after the bubbles were driven away. The glass slide was then dragged out and dried in the incubator at 37°C, dewaxed normally. The tissue slices were then washed with water for 10 min and soaked in 3%H2O2 solution for 10 min followed by washed by water twice. Citrate buffer was added and the slide was stewed under medium-fire option in a microwave oven till boiling and then cooled and heated till boiling for the second time. After cooling to room temperature, the citrate buffer was dumped and water washed the slide for twice and then PBS washed the slide twice for 5 min. After cleaning PBS around the tissues, 900μl PBS and100μl FBS (Cat#:20140421, Gibco, USA) was immediately used to seal the locus. Primary antibodies against CD34(μg/ml, ab237972) and VEGFR2(1:70, ab39638) were commercially provided by Abcam, Shanghai, China. After cleaning the serum around the tissue samples, the primary antibody solution was added after respective dilution separately and the slides were put into a fridge at 4°C for a night. The second day, the secondary antibody IgG H&L (HRP) (ab6721, 1:1000, Abcam, Shanghai, China) was added after the slides were washed using PBS for three times and the slides were then kept in an incubator at 37°C for half an hour. DAB kit was used to color the antigens in tissue samples and operated under microscope (ZSGB, Beijing, China). Hematoxylin was then added to redye the nuclear (Beyotime, Shanghai, China). The slides were washed with water and then soaked in alcohol with increasing concentrations (50%, 70%, 85%, 95% and 100%) for 1 min respectively. Neutral balsam was dripped to seal the slides. Inverted microscope was used to observe the stained tissue samples and images were taken and IOD values were evaluated using Image J tool (NIH, USA).

EPC separation and culture

All the mice were executed by cutting the necks and then were put in 75% alcohol for 5 min. Under aseptic condition, we separated the thighbone and wiped out the muscle tissues. 1 ml DMEM/F12 was injected into the one end of the thighbone to wash for three times and the bone marrow tissues were washed out and then grinded using 200-mesh stainless steel screen in order to split the tissues into cells. 2ml DMEM/F12 serum-free culture was used to centrifuge the cells and the supernatant was abandoned and then 2ml DMEM/F12 resuspended cells and then were added into the lymphocyte separating medium and centrifuged at 1500r/min for 30 min. Pipet aspirated the cloud-like cell band in middle. Cells were washed with DMEM/F12 twice and cultured at 37°C with 5% CO_2. The medium was changed every three

days. After 14 days, the cells grew and merged to 80%-90% as observed under microscope. Cellular morphology was imaged under microscope.

Immunofluorescence method for CD34+ and VEGFR2+ cells identification

Cells at logarithmic phase were seeded onto 24-well plates and cultured for 24h in the incubator at 37°C with 5% CO_2. PBS washed cells twice and after aspiration of PBS，300μL 4% triformol was used to fix the cells. After 30min, cold PBS washed the cells for three times (5 min each time). 300 μL 0.05% Triton-X -100 (diluted with PBS) was added into each well and the plate was put still at 4°C for 5 min. Thereafter, 300 μL 10% donkey serum (Gibco, USA) was added into each well for 2h after cells were washed 3 times using cold PBS. The primary antibodies were diluted using 1% donkey serum. 300 μL primary antibodies after dilution was added into each well overnight at 4°C. The primary antibodies were exactly the same ones used above. The second day, after the plate was taken out and put still at room temperature for 30min, cold PBS washed cells for three times (5 min each time). 300μL 1% IgG H&L(FITC) antibody (ab7079, Abcam, Shanghai, China) after diluted with PBS was added into each well and the culture was incubated for 2h at 4°C. Thereafter, the cells were washed using cold PBS for three times and then 300 μL DAPI (1:1000 dilution rate and the final concentration, 1 μg/ml) was added into each well and the plate was incubated for 5 min at 4°C. Cold PBS washed cells for three times and 3μl protective agent was dropped on the slides and the fluorescence was observed and pictured under the fluorescence microscope.

Cell treatment

EPCs at logarithmic phase from the blank, CAS Control, SIRT1 inhibitor and SIRT1 agonist groups were selected for further study and cells from the Control group was further treated with autophagy inhibitor 3Ma (5mmol/L) or wnt pathway inhibitor IWP-2(20umol/L) for 12h. Cells from Control, 3Ma and IWP-2 groups are ready for further analysis.

RT-PCR

Cells were seeded into 6-well plates for RT-PCR assay. Total RNAs were extracted by adding 1ml Trizol (R0016, Beyotime, Shanghai, China) into each well according to producer's recommendations. cDNA was synthesized using BeyoRT™ III cDNA (Beyotime, Shanghai, China). SYBR Premix Ex Taq Kit was used to measure the relative expression of SIRT1 against internal control of β-actin . The primer sequence was listed (Table1). Each group was detected for three repeated times. The $2^{-\Delta\Delta Ct}$ method quantified the relative expression levels in each group.

MTT

Cells were planted into 96-well plates. After cultured for 24, 48 and 72h, cell culture in the plates were added with MTT solution (Beyotime, diluted to 5mg/ml MTT solution,10ul per well). The plates were incubated for another 4 hours. Thereafter, 100ul Formazan was added into each well of the plate and the

cell culture continued till the Formazan was totally dissolved as confirmed under microscope observation. OD values were measured at the wavelength of 570nm using a micro-plate reader. Each group was repeated for three independent times.

Colony formation

Cell culture medium was abandoned and cells were thereafter washed with PBS. 0.02 EDTA and 0.25% trypsin was added into each well for digestion. DMEM with 10%FBS was added to stop the trypsinization. 200 cells from each group were seeded into the 12-well plates, complemented with 2 ml complete medium. The plates were incubated at 37℃ and under 5%CO2 environment for 1-2 weeks. When the cell number in each colony reached 50 at least, the complete medium was abandoned and PBS embathed the cells. 500ul 4% paraformaldehyde was used to fix the cells and the plates were incubated for another 30 min at 4℃. After cells were washed again using PBS, 500ul 0.1% crystal violet was added into each well. After the plates dried, colony images were taken on a Huawei smart phone. All the experiments were done for three times. Colony numbers were counted and further analyzed using Graphpad 8 (Graphpad Prism, CA, USA).

Scratch

Cells were collected from each group and incubated in 96-well plates (10^5). Wounds in parallel were generated using a 20-μl pipette. PBS washed the scratched cells away and then serum-free medium was added and the plates were incubated at 37°C with 5% CO_2. Images were taken at 0, 24,48h and Image J was used to analyze the scratch width and relative migration distances at 24h and 48h were calculated based on the width values measured at 0,24,48h. Each group was evaluated for three independent times.

Western Blot

RIPA was added into the cell culture to lyse the cells (Beyotime, Shanghai, China). Then we centrifuged the cells and collected supernatants. Proteins were segregated utilizing SDS-PAGE and thereafter transferred to PVDF membrane（Beyotime, Shanghai, China）. The membranes were put into Blotto, shaken and blocked for 2h at room temperature and blotted. The primary antibodies were added into Blotto solution and the membranes were incubated in the mixed culture and incubated overnight at 4℃. After this, the membranes were put in 1X TBST solution and rinsed shaking for 5 min for 4 times. HRP IgG antibody was used as a secondary antibody and mixed in Blotto. The membranes were incubated inside the mixture for 1.5h at room temperature. ECL was used to develop and film the blots of the immunoreactive proteins. Image J Software (NIH, USA) analyzed the relative grey values of the blots against GADPH. The antibodies were used after diluted as below.

Statistical analysis

Statistical presentations were presented in bar or line graphs using mean and standard deviation (sd) values derived from three repetitions of each experiment. Graphpad 8 (Graphpad Prism, CA, USA) was

used to perform all the analysis. Single comparison between two groups was analyzed using student-t method while multiple comparisons were made among different groups based on mean and sd values of the results in each group using One-way ANOVA method (for single index) together with Tukey's multiple comparison test while using Two-way ANOVA method (for multiple index) coupled with Sidak's multiple comparison test in weight curve, MTT viability analysis. General alpha level is set 0.05.

Results

SIRT1 activator alleviated pathogenesis in CAS mice and induced higher CD34+/VEGFR2+ in coronary artery

CAS animal model was established through constant high fat feeding on ApoE-/- mice with the C57BL/6 mice as the blank control. In addition, SIRT1 expression was regulated in CAS via injection of SIRT1 activator or inhibitor. It was found that mice were significantly heavier in CAS model (Control) than those in the blank group (Figure 1A). Furthermore, SIRT1 agonist resulted in the weight decrease in mice(Figure 1A). On the contrary, SIRT1 inhibitor led to the weight growth in mice (Figure 1A). Differential treatments of mice also changed the lipids in serum. It was discovered that the TC,TG、LDL levels in CAS mice were higher than the blank group while SIRT1 inhibitor induced even higher lipid levels of TC,TG、LDL in CAS mice and SIRT1 activator attenuated the high lipid levels in CAS mice (Figure 1B,C,E) .HDL levels were detected to be lower in CAS mice and the activation of SIRT1 partly restored the HDL serum levels in CAS mice (Fig1D). The observations from weight and lipid modulations suggested the formation of CAS mice model as well. To further validate this, H&E staining and IHC methods were performed on the tissue samples of coronary artery dissected from each mouse from all groups. HE staining results displayed the significant lesion area in CAS group compared to the healthy control (Figure 1F) while the SIRT1 involvement could modulate the lesion size, which specifically supported that the SIRT1 inhibitor could aggravate the lesion （SIRT1 in vs Control, Figure 1F） and activation of SIRT1 could shrink the lesion size and alleviate the pathological syndrome in CAS mice (SIRT1 ago Vs Control, Figure 1F). IHC methods targeted the EPC cellular surface markers, CD34 and VEGF2R and results showed that the density of CD34+/VEGFR2+ was significantly enhanced in coronary artery in CAS mice in comparison with the blank healthy group (Fig1G) while the density was associated with the SIRT1 modulation in CAS mice, which is that SIRT1 inhibition led to higher CD34+/VEGFR2+ expression and activator inhibited in part CD34+/VEGFR2+ (Figure 1G-H）, suggesting a possibility that CD34+/VEGFR2+ was related to the lesion severity and the more serious the lesions were, higher CD34+/VEGFR2+ expression was, perhaps acting the reparative role and neovascular functions. Taken together, in vivo, we presented that SIRT1 activation alleviated the CAS lesion and serum lipid conditions, perhaps by activating higher CD34+/VEGFR2+ in the lesion areas in coronary artery in mice.

EPC separation, culture and identification

EPCs were separated from bone marrows of the mice (Figure 2A) and then cultured as described above in methods. Cellular morphology was imaged under microscope on Day4, 7, 14 and 21 and it was noted that

cells grew into spindle shapes (Figure 2B). Immunofluorescence assays disclosed the subcellular localization of CD34 and VEGFR2 and images showed that CD34 didn't exist in nuclear while VEGFR2 showed up in both nuclear and cytoplasma, which was generally in accordance with the protein characteristics of CD34 and VEGFR2(UniProt, https://www.uniprot.org/uniprot/Q64314) (Figure 2C-D).

SIRT1 activated the EPC proliferation and migration in vitro

After separation and identification of the EPCs collected from the mice in blank, control, SIRT1 inhibitor and SIRT1 agonist groups. SIRT1 expression was detected by RT-PCR in each group mentioned above as well as in additional two groups where cells were treated with autophagy inhibitor 3-MA or the signaling inhibitor IWP-2 and the results were valid (Figure 3A). RT-PCR further confirmed that SIRT1 expression was lower in the Control group than the blank group while SIRT1 expression was considerably higher in SIRT1 agonist group and lower in SIRT1 inhibitor group with the Control group as a reference (Figure 3B). The bone marrow-derived EPCs were then selected for RNA viability and colony formation assays. The findings indicated that SIRT1 activation increased EPC viability and colony capability (Figure3A-B). Scratch methods showed that the EPCs contained lower migration capability in the Control group than those in the blank group while SIRT1 activation in EPCs restored the migration property and inhibitor of SIRT1 discouraged EPC migration, which was in accordance with proliferation (Figure 3E-G).

SIRT1 activation inhibited EPC autophagy, promoted proliferation and migration and triggered the wnt/β-catenin/GSK3β signaling pathway

Western blot methods analyzed the protein changes of autophagy markers ATG1, LC3II and signaling markers, wnt5a, β-catenin and phosphor-GSK3β, GSK3β with GAPDH as the internal control. Results showed that ATG1 and LC3II were activated in EPCs from CAS control group compared to the blank group while SIRT1 agonist could inhibit the protein levels of ATG1 and LC3II, signifying that the autophagy could be inhibited by SIRT1 activation in EPCs (Figure 4A, B, C). In addition, it was also indicated that wnt5a/β-catenin/GSK3β were inhibited in the control group compared to the blank and restored in SIRT1 agonist group (Figure 4A, D, E, F).

Autophagy inhibitor 3Ma induced the SIRT1 activation in EPCs, promoted cell proliferation, migration and activated the wnt/β-catenin/GSK3β signaling pathway

EPCs in the control group were cultured with the addition of autophagy inhibitor, 3Ma. Thereafter, RT-PCR evaluated the SIRT1 expression in cells in 3Ma group in comparison with the control group and it was found that SIRT1 mRNA expression was elevated by 3Ma treatment (Figure 5A). MTT assays showed that EPC viability was enhanced by 3Ma addition and Colony formation supported this in terms of colony number (Figure 5B, C). Western Blot analyzed the protein changes with regards to the wnt/β-catenin/GSK3β signaling pathway, which showed that wnt5a, β-catenin protein expression was significantly promoted as well as the ratio of phosphor-GSK3β/ GSK3β, displaying the promotive effect of 3Ma on the signaling pathway (Figure 5D-G). Similarly, it was also confirmed by scratch assays that autophagy inhibition could add to EPC migration (Figure 5H-J).

Wnt inhibitor could induce autophagy and inhibit EPC proliferation and migration

The EPCs from the control group were selected for further treatment by wnt/β-catenin/GSK3β signaling inhibitor, IWP-2. SIRT1 was discovered to be suppressed in EPCs after IWP-2 treatment according to RT-PCR results (Figure 6A). IWP-2 addition also led to a decrease in colonies and viability of EPCs (Figure 6B-C). In addition, IWP-2 also resulted in ATG1 and LC3II activation in EPCs (Figure 6D). EPC migration ability was inhibited by IWP-2 as well (Figure 6E-G).

Discussion

EPCs, featured by surface protein markers CD34, VEGFR2, or CD133, mainly exist in bone marrows and circulating blood in humans and animals[19, 20]. EPCs can differentiate into endothelial cells forming all endothelium, exerting the regeneration and reparative function[21]. When endothelial integrity is disturbed, EPCs migrate from bone marrow to repair the endothelium through proliferation and differentiation[22]. Thus, EPCs have been tried in vitro and in vivo even in clinical stage as potential therapeutic strategies in intracerebral hemorrhage[23], chronic kidney diseases[24], diabetes[25], etc. A recent study further revealed that high EPCs could predict a better prognosis in CAS patients based on 10-year follow-up analysis, which largely agreed with an earlier 5-year follow-up study[8, 26]. Clinically, it was reported that the number of circulating EPCs was negatively associated with risks of the cardiovascular events[27] while in stented coronary artery tissues, EPC counts were negatively related to plaque area in patients, which might counteract with each other [28]. An interesting study further reported that in Coronary artery disease patients, EPC counts in the myocardial tissue were correlated with the severity of the disease[29]. These two findings might disagree with many previous ones, however, catching our attention. Therefore, in our animal experiments, we mimicked CAS in ApoE-/- mice, fed by high-fat diet and evaluated the relative density of CD34+/VEGFR2+ in the coronary artery tissues of CAS mice and normal mice by IHC methods, which demonstrated that the EPCs density was higher in CAS mice rather than normal mice. This was in accordance in the findings in humans with similar diseases. To get a deeper understanding of this, we further did in-vitro assays using the EPCs derived from bone marrows of the mice and found that EPCs from CAS mice presented lower proliferation and migration than the normal mice. Considering that bone marrows are one of the major sources to provide EPCs and enable EPC homing to injured endothelium[30], we supposed that the lower proliferation and migration of EPCs in CAS group manifested the general conditions of the disease, which was similar to the previous findings in human being[31, 32]. Previous clinical findings suggested that SIRT1 might be protective in CAS patients and in vitro, it could regulate EPC senescence, proliferation, migration and angiogenesis in an oxidative stress cellular model [33].

In cellular level, it was reported previously that EPC autophagy was associated with proliferation[34]. Transcription factor E2-2 was discovered to obstruct EPC proliferation via autophagy suppression[35]. SIRT1 could promote the EPCs proliferation in vitro[36]. Yet, few previous studies explored the autophagy-regulated proliferation of EPCs in the context of CAS. Moreover, there is absence of the specific regulatory mechanism and lack of in vivo proof for SIRT1 regulation in CAS. Therefore, we investigated this in vivo

through SIRT1 activator or inhibitor manipulation on mice and in EPCs separated from mice and thereafter treated by autophagy inhibitor 3Ma. In vivo, it was discovered that SIRT1 activator alleviated the lesions, improved the HDL level and activated EPC biomarkers, CD34+/VEGFR2+ in coronary artery tissues of the CAS mice. In vitro, SIRT1 activator induced EPCs proliferation and migration, obstructed autophagy. 3Ma inhibited EPC autophagy and was discovered to promote EPC proliferation and migration. Therefore, we presented in bone marrow-derived EPCs, autophagy inhibition could promote cell proliferation and migration. It was also discovered that SIRT1 expression was elevated by autophagy inhibition in EPCs. Therefore, we concluded that autophagy inhibitor, SIRT1 might contribute to alleviation in CAS in mice perhaps by recruiting the circulating EPC homing to injured areas of coronary artery and autophagy inhibition might help to fuel EPC proliferation from bone marrow and increase EPC migration.

As formerly reported, AKT pathway was involved in the regulatory system of EPC proliferation and autophagy[34]. Endothelial nitric oxide synthesis (eNOS) was revealed to modulate the cell migration, proliferation and mobility in EPCs via Pi3k/AKT pathway[37, 38]. However, there is little research on the further mechanisms related to EPC autophagy. Wnt/β-catenin/GSK3β signaling is a classic pathway in cellular function mediations and it was reported that inhibition in upstream of Wnt signaling was associated with autophagy activation in colorectal cancer cells[39]. An earlier study disclosed in detail that β-catenin could bind LC-3 and inhibit the formation of autophagosomes and modulate P62 in colorectal cancer cells [40]. Similarly, in glioma cells, wnt/β-catenin signaling exerted its inhibitory effect on tumor cell autophagy[41]. Despite wnt/β-catenin modulated the cellular autophagy in tumors, there is no report on EPC autophagy and wnt/β-catenin signaling pathway yet. Therefore, we further investigated the potential role of wnt/β-catenin signaling pathway in EPCs functions. GSK3β was able to modulate the mTORC1 to suppress autophagy in cancer cells[42]. We researched on wnt/β-catenin/GSK3β signaling in EPCs. We noted that in CAS control group, the signaling was inactivated compared to the blank group and SIRT1 activator could reactivate the signaling pathway. In addition, after autophagy inhibition, the signaling was considerably restored. On the other hand, when IWP-2 was introduced to inhibit the signaling pathway, it was observed that EPC proliferation and migration was decreased while autophagy was promoted.

Therefore, in conclusion, SIRT1 activator, might help to alleviate CAS severity in mice via accelerating the EPCs homing to the injured areas in coronary artery segments. In vitro, SIRT1 activator could promote the EPCs proliferation, migration and inhibit autophagy via wnt/β-catenin/GSK3β signaling pathway.

Declarations

Author contributions

Yanwei L- Literature search, DesignData, analysis, Statistical analysis, Manuscript review

Wei Cui- Concepts, Design, Data acquisition, Manuscript editing

Bing Song- Definition of intellectual content, Literature search

Xuying Ye- Experimental studies

Zhuqing Li- Manuscript preparation

Chengzhi Lu- Manuscript preparation, Manuscript review, Guarantor

- **Funding:** No funding was granted for this study at any stage of work.

- **Conflict of Interest:** No conflict of interest was found or declared by any of authors.
- **Ethics approval and consent to participate**

Ethical approval was obtained from Institutional ethical review Board (IEC) of The First Affiliated Hospital of Jinzhou Medical University, Jinzhou City, Liaoning Province, China. Informed consent was obtained from the participants with the option to withdraw them from the study at any time.

- **Consent for publication**

IEC of The First Affiliated Hospital, Jinzhou City, Liaoning Province, China affiliated to of Jinzhou Medical University, approved the publication of data generated from this study.

- **Availability of data and material**

All data are provided in this study and raw data can be requested to corresponding author.

References

1. Tesfamariam B. Endothelial Repair and Regeneration Following Intimal Injury. J Cardiovasc Transl Res. 2016;9:91–101.
2. Watt J, Kennedy S, Ahmed N, Hayhurst J, McClure JD, Berry C, et al. The relationship between oxidised LDL, endothelial progenitor cells and coronary endothelial function in patients with CHD. Open heart. 2016;3:e000342.
3. Huang PH, Chen JW, Lin SJ. Effects of Cardiovascular Risk Factors on Endothelial Progenitor Cell. Acta Cardiologica Sinica. 2014;30:375–81.
4. Blum A, Adawi M. Rheumatoid arthritis (RA) and cardiovascular disease. Autoimmun rev. 2019;18:679–90.
5. Lee PS, Poh KK. Endothelial progenitor cells in cardiovascular diseases. World journal of stem cells. 2014;6:355–66.
6. Fujita Y, Kawamoto A. Stem cell-based peripheral vascular regeneration. Adv Drug Deliv Rev. 2017;120:25–40.
7. Alexandru N, Safciuc F, Constantin A, Nemecz M, Tanko G, Filippi A, et al. Platelets of Healthy Origins Promote Functional Improvement of Atherosclerotic Endothelial Progenitor Cells. Front Pharmacol. 2019;10:424.

8. Pelliccia F, Pasceri V, Moretti A, Tanzilli G, Speciale G, Gaudio C. Endothelial progenitor cells predict long-term outcome in patients with coronary artery disease: Ten-year follow-up of the PROCREATION extended study. Int J Cardiol. 2020;318:123–5.
9. Ndunda P, Vindhyal MR, Muutu T, Fanari Z. Clinical Outcomes of the Dual-Therapy CD34 Antibody-Covered Sirolimus-Eluting Stent Versus Standard Drug-Eluting Coronary Stents: A Meta-Analysis. Cardiovascular revascularization medicine: including molecular interventions. 2020;21:213–21.
10. Ravindranath RR, Romaschin A, Thompson M. In vitro and in vivo cell-capture strategies using cardiac stent technology - A review. Clinical biochemistry. 2016;49:186–91.
11. He X, Zheng J, Liu C. Low serum level of sirtuin 1 predicts coronary atherosclerosis plaques during computed tomography angiography among an asymptomatic cohort. Coron Artery Dis. 2019;30:621–5.
12. Breitenstein A, Wyss CA, Spescha RD, Franzeck FC, Hof D, Riwanto M, et al. Peripheral blood monocyte Sirt1 expression is reduced in patients with coronary artery disease. PloS one. 2013;8:e53106.
13. Hsu CP, Odewale I, Alcendor RR, Sadoshima J. Sirt1 protects the heart from aging and stress. Biological chemistry. 2008;389:221–31.
14. Wang YQ, Cao Q, Wang F, Huang LY, Sang TT, Liu F, et al. SIRT1 Protects Against Oxidative Stress-Induced Endothelial Progenitor Cells Apoptosis by Inhibiting FOXO3a via FOXO3a Ubiquitination and Degradation. Journal of cellular physiology. 2015;230:2098–107.
15. Zha S, Wang F, Li Z, Ma Z, Yang L, Liu F. PJ34, a PARP1 inhibitor, promotes endothelial repair in a rabbit model of high fat diet-induced atherosclerosis. Cell cycle (Georgetown Tex). 2019;18:2099–109.
16. Jiang Q, Hao R, Wang W, Gao H, Wang C. SIRT1/Atg5/autophagy are involved in the antiatherosclerosis effects of ursolic acid. Molecular cellular biochemistry. 2016;420:171–84.
17. Hassanpour M, Rezabakhsh A, Pezeshkian M, Rahbarghazi R, Nouri M. Distinct role of autophagy on angiogenesis: highlights on the effect of autophagy in endothelial lineage and progenitor cells. Stem Cell Res Ther. 2018;9:305.
18. Wang C, Mao C, Lou Y, Xu J, Wang Q, Zhang Z, et al. Monotropein promotes angiogenesis and inhibits oxidative stress-induced autophagy in endothelial progenitor cells to accelerate wound healing. J Cell Mol Med. 2018;22:1583–600.
19. Rana D, Kumar A, Sharma S. Endothelial Progenitor Cells as Molecular Targets in Vascular Senescence and Repair. Curr Stem Cell Res Therapy. 2018;13:438–46.
20. Peters EB. Endothelial Progenitor Cells for the Vascularization of Engineered Tissues. Tissue engineering Part B Reviews. 2018;24:1–24.
21. Heidarzadeh M, Roodbari F, Hassanpour M, Ahmadi M, Saberianpour S, Rahbarghazi R. Toll-like receptor bioactivity in endothelial progenitor cells. Cell tissue research. 2020;379:223–30.
22. Guerra G, Perrotta F, Testa G. Circulating Endothelial Progenitor Cells Biology and Regenerative Medicine in Pulmonary Vascular Diseases. Curr Pharm Biotechnol. 2018;19:700–7.

23. Pías-Peleteiro J, Campos F, Perez-Mato M, Lopez-Arias E, Rodriguez-Yanez M, Castillo J, et al. Endothelial Progenitor Cells as a Therapeutic Approach for Intracerebral Hemorrhage. Curr Pharm Design. 2017;23:2238–51.
24. Coppolino G, Cernaro V, Placida G, Leonardi G, Basile G, Bolignano D. Endothelial Progenitor Cells at the Interface of Chronic Kidney Disease: From Biology to Therapeutic Advancement. Curr Med Chem. 2018;25:4545–51.
25. Pyšná A, Bém R, Němcová A, Fejfarová V, Jirkovská A, Hazdrová J, et al. Endothelial Progenitor Cells Biology in Diabetes Mellitus and Peripheral Arterial Disease and their Therapeutic Potential. Stem cell reviews reports. 2019;15:157–65.
26. Pelliccia F, Pasceri V, Rosano G, Pristipino C, Roncella A, Speciale G, et al. Endothelial progenitor cells predict long-term prognosis in patients with stable angina treated with percutaneous coronary intervention: five-year follow-up of the PROCREATION study. Circulation journal: official journal of the Japanese Circulation Society. 2013;77:1728–35.
27. Werner N, Kosiol S, Schiegl T, Ahlers P, Walenta K, Link A, et al. Circulating endothelial progenitor cells and cardiovascular outcomes. N Engl J Med. 2005;353:999–1007.
28. Otto S, Nitsche K, Jung C, Kryvanos A, Zhylka A, Heitkamp K, et al. Endothelial progenitor cells and plaque burden in stented coronary artery segments: an optical coherence tomography study six months after elective PCI. BMC Cardiovasc Disord. 2017;17:103.
29. Morrone D, Felice F, Scatena C, De Martino A, Picoi MLE, Mancini N, et al. Role of circulating endothelial progenitor cells in the reparative mechanisms of stable ischemic myocardium. Int J Cardiol. 2018;257:243–6.
30. Hristov M, Erl W, Weber PC. Endothelial progenitor cells: mobilization, differentiation, and homing. Arteriosclerosis, thrombosis, and vascular biology. 2003;23:1185–9.
31. Balbarini A, Barsotti MC, Di Stefano R, Leone A, Santoni T. Circulating endothelial progenitor cells characterization, function and relationship with cardiovascular risk factors. Curr Pharm Design. 2007;13:1699–713.
32. Hammadah M, Samman Tahhan A, Mheid IA, Wilmot K, Ramadan R, Kindya BR, et al. Myocardial Ischemia and Mobilization of Circulating Progenitor Cells. Journal of the American Heart Association. 2018;7:e007504.
33. Lamichane S, Baek SH, Kim YJ, Park JH, Dahal Lamichane B, Jang WB, et al. MHY2233 Attenuates Replicative Cellular Senescence in Human Endothelial Progenitor Cells via SIRT1 Signaling. Oxidative medicine and cellular longevity. 2019;2019:6492029.
34. Xiao J, Lu Y, Yang X. THRIL mediates endothelial progenitor cells autophagy via AKT pathway and FUS. Molecular medicine (Cambridge, Mass). 2020;26:86.
35. Zhang L, Yu Y, Xia X, Ma Y, Chen XW, Ni ZH, et al. Transcription factor E2-2 inhibits the proliferation of endothelial progenitor cells by suppressing autophagy. Int J Mol Med. 2016;37:1254–62.
36. Ming GF, Wu K, Hu K, Chen Y, Xiao J. NAMPT regulates senescence, proliferation, and migration of endothelial progenitor cells through the SIRT1 AS lncRNA/miR-22/SIRT1 pathway. Biochem Biophys

Res Commun. 2016;478:1382–8.

37. Walter DH, Zeiher AM, Dimmeler S. Effects of statins on endothelium and their contribution to neovascularization by mobilization of endothelial progenitor cells. Coron Artery Dis. 2004;15:235–42.
38. Everaert BR, Van Craenenbroeck EM, Hoymans VY, Haine SE, Van Nassauw L, Conraads VM, et al. Current perspective of pathophysiological and interventional effects on endothelial progenitor cell biology: focus on PI3K/AKT/eNOS pathway. Int J Cardiol. 2010;144:350–66.
39. Wang J, Ren XR, Piao H, Zhao S, Osada T, Premont RT, et al. Niclosamide-induced Wnt signaling inhibition in colorectal cancer is mediated by autophagy. Biochem J. 2019;476:535–46.
40. Petherick KJ, Williams AC, Lane JD, Ordóñez-Morán P, Huelsken J, Collard TJ, et al. Autolysosomal β-catenin degradation regulates Wnt-autophagy-p62 crosstalk. EMBO J. 2013;32:1903–16.
41. Nàger M, Sallán MC, Visa A, Pushparaj C, Santacana M, Macià A, et al. Inhibition of WNT-CTNNB1 signaling upregulates SQSTM1 and sensitizes glioblastoma cells to autophagy blockers. Autophagy. 2018;14:619–36.
42. Azoulay-Alfaguter I, Elya R, Avrahami L, Katz A, Eldar-Finkelman H. Combined regulation of mTORC1 and lysosomal acidification by GSK-3 suppresses autophagy and contributes to cancer cell growth. Oncogene. 2015;34:4613–23.

Tables

Table 1. Primer sequences

SIRT1	Forward 5’-CAGGTTGCAGGAATCCAAA3’;
SIRT1	Reverse 5’-CAAATCAGGCAAGCTGCTGT3
β -actin	Forward 5’-TCAAGATCATTGCTCCTCCTGAG3’
β -actin	Reverse, 5’-CTGCTTGCTGATCCACATCTG3’

Table 2. Primary antibodies used in this study.

Antibodies	Source (dilution rate, item ID, company)
ULK1（ATG1）	1 μg/mL, ab167139, Abcam
LC3II	1:2000, ab192890，Abcam
Wnt5a	1:1000, ab229200, Abcam
Beta-catenin	1:1000, ab227499, Abcam
Phosphor-GSK3β	1:5000, ab32391, Abcam
GSK3β	1:2000, ab93926, Abcam
β-actin	1:2500, ab8227, Abcam

Figures

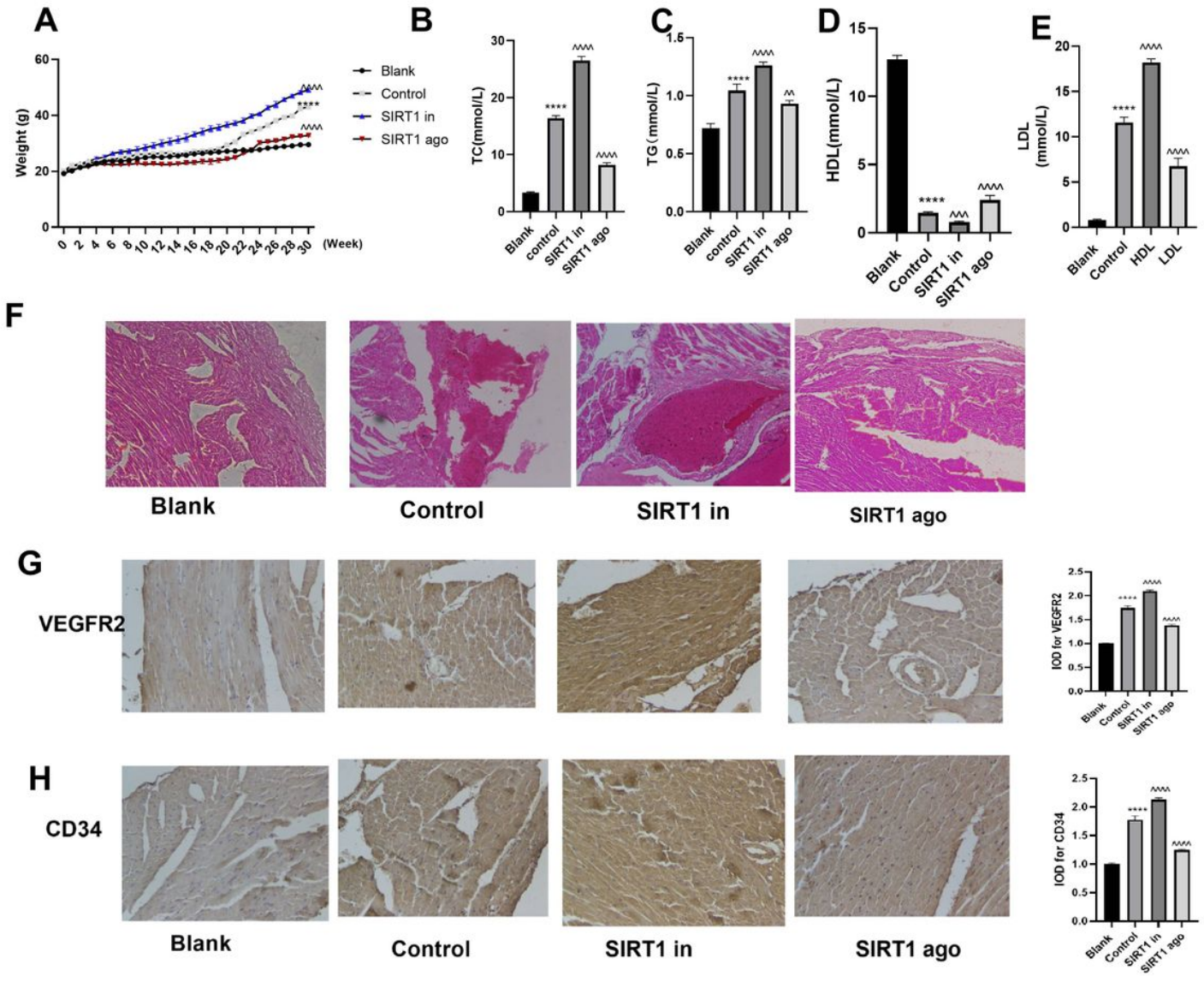

Figure 1

SIRT1 activator inhibited the LDL serum level, increased HDL serum level, alleviated pathological lesions and lower CD34+/VEGFR2+ expression in CAS mice coronary arteries CAS animal model was established through constant high fat feeding on ApoE-/- mice with the C57BL/6 mice as the blank control. In addition, SIRT1 expression was regulated in CAS via SIRT1 activator or inhibitor. A. weights of all mice were measured on a weekly base and mean and sd values were presented in the line charts. B-E. Serum lipid levels were detected in the blood, sampled from the postorbital venous plexus were detected using medical automatic biochemical analyzer (Hitachi, Tokyo, Japan) at Week 30 before sacrifice. Mean and sd values were shown in the bar graphs. F. H&E staining was used to observe the lesion changes in CAS mice in response to SIRT1 inhibitor or agonist. G-H. IHC methods were used to track the EPC surface

protein makers, CD34 and VEGFR2 in response to SIRT1 regulation in mice. ****P<0.0001, Control Vs Blank, ^^^^P<0.0001, ^^^P<0.001, ^^P<0.01, Vs Control.

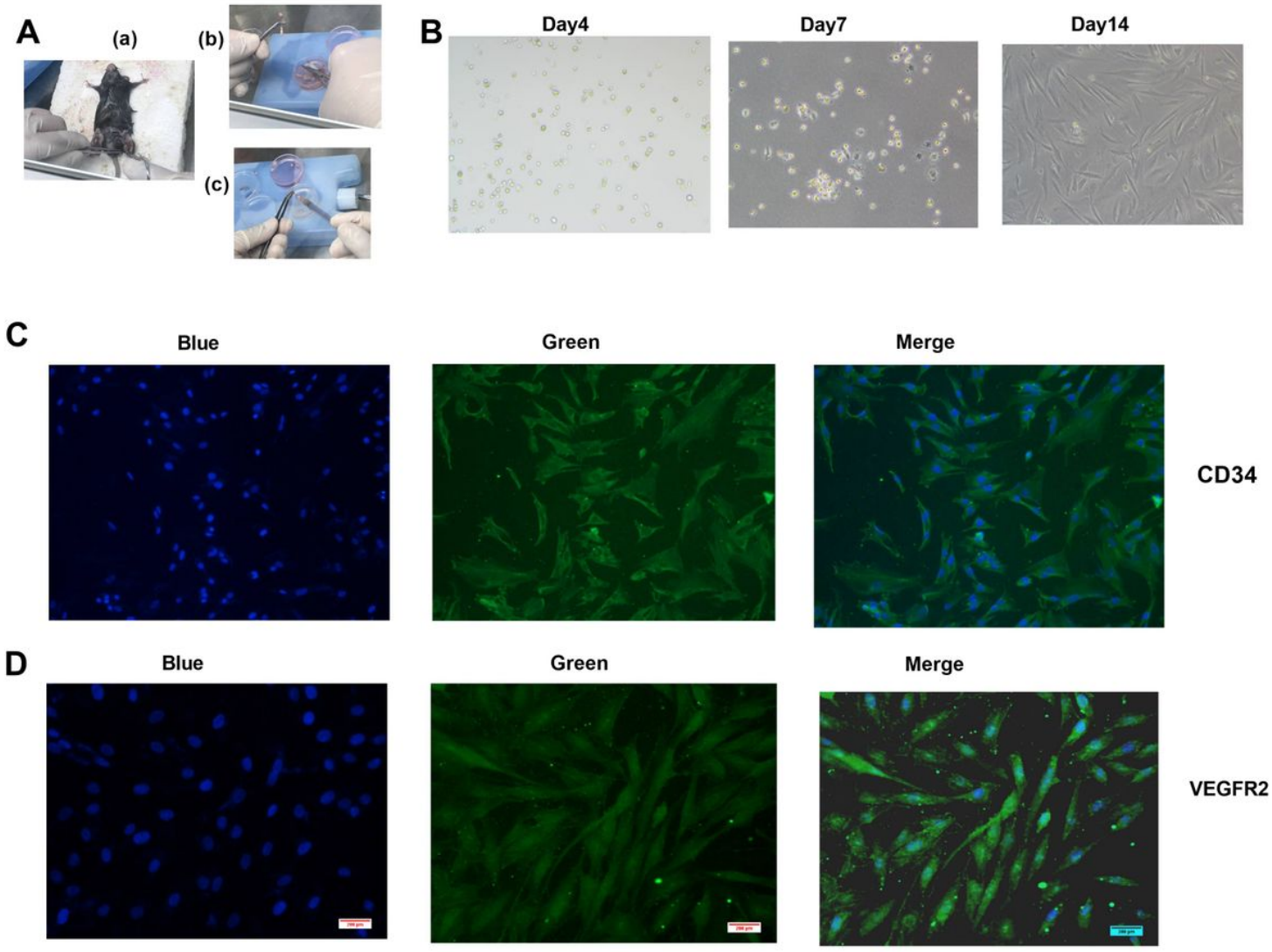

Figure 2

EPC separation, culture and identification. A. EPCs were separated from bone marrows of the mice and then cultured as described above in methods. B. Cellular morphology was imaged under microscope on Day4, 7, 14 and 21. C-D. Immunofluorescence assays disclosed the subcellular localization of CD34 and VEGFR2.

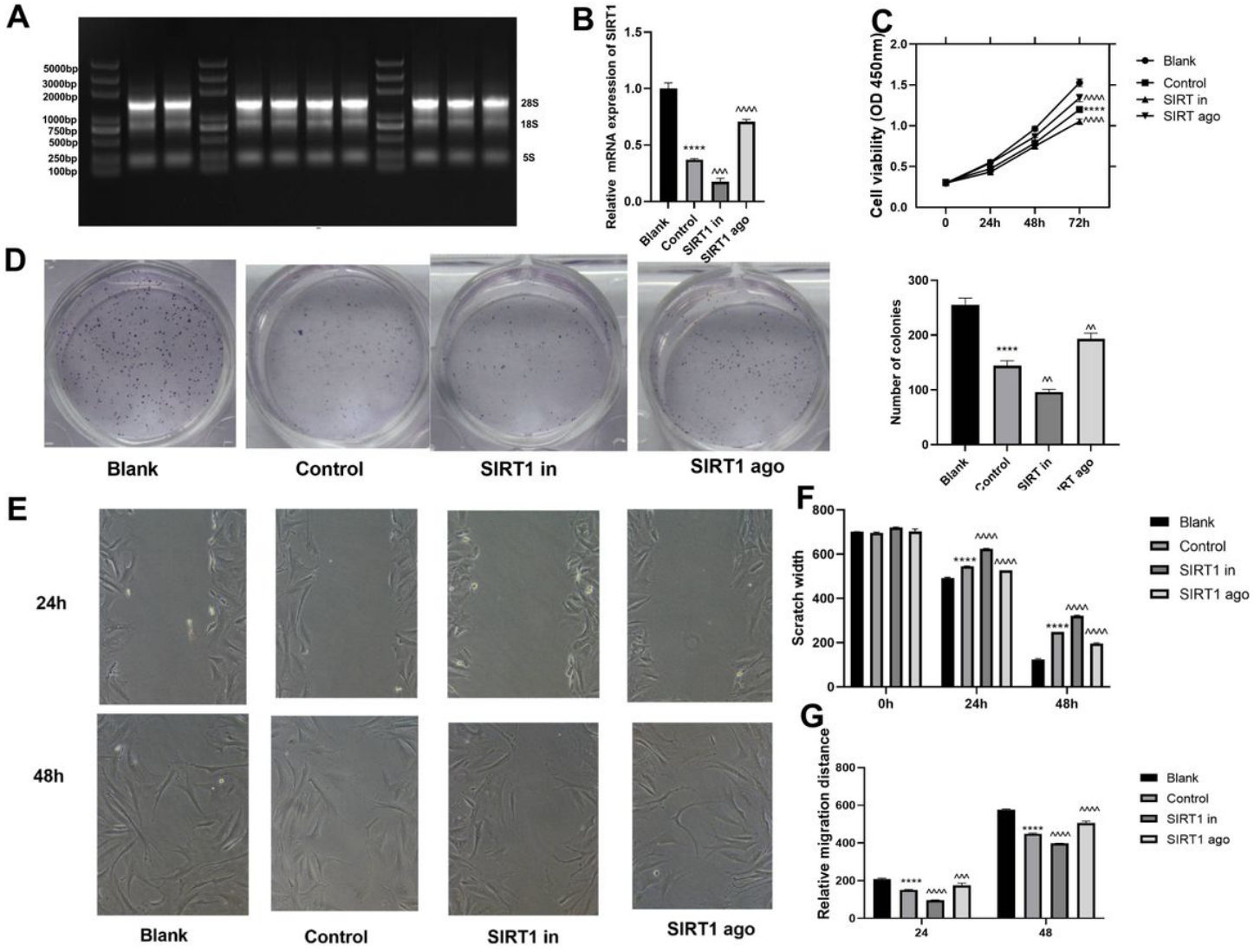

Figure 3

SIRT1 activation promoted the EPC proliferation and migration in vitro A. RNA extraction for all groups. B. RT-PCR methods detected SIRT1 expression in EPCs. C-D.Cells were selected for viability and colony formation assays.E, Scratch results at 24h, 48h. F. Scratch width. G,Relative migration distance at 24h and 48h. ****P<0.0001, ***P<0.001, **P<0.01, *P<0.05. Control Vs Blank, ^^^^P<0.0001, ^^^P<0.001, ^^P<0.01, ^P<0.05, Vs Control.

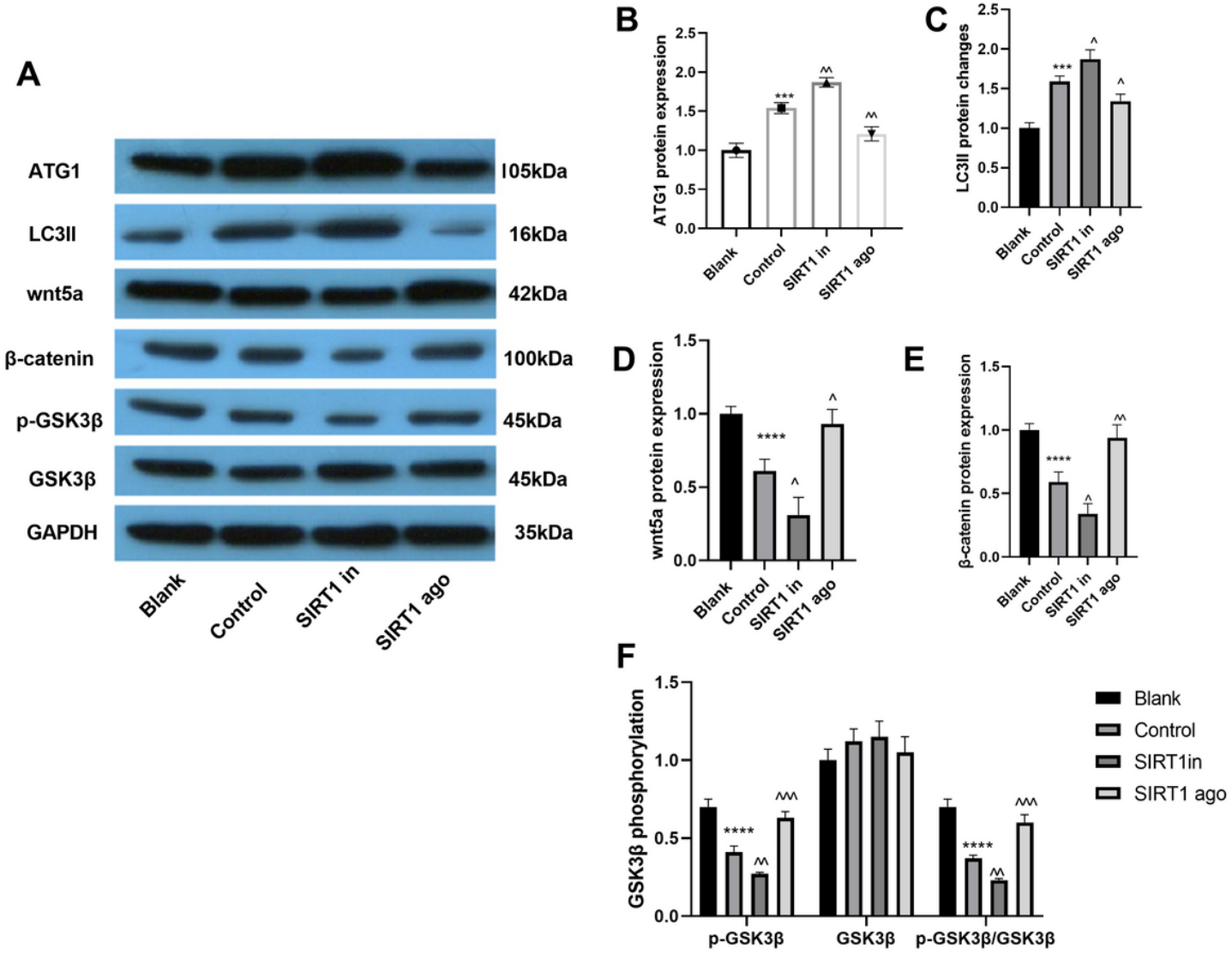

Figure 4

SIRT1 activation induced EPC autophagy and triggered the β-catenin/GSK3β signaling pathway Western blot analyzed the the protein changes of autophagy markers ATG1, LC3II and signaling markers, wnt5a, β-catenin and phosphor-GSK3β, GSK3β with GAPDH as the internal control. Image J was used to quantify the protein density of each group with an internal reference to B-ACTIN. ****P<0.0001, ***P<0.001, **P<0.01, *P<0.05. Control Vs Blank, ^^^^P<0.0001, ^^^P<0.001, ^^P<0.01, ^P<0.05, Vs Control.

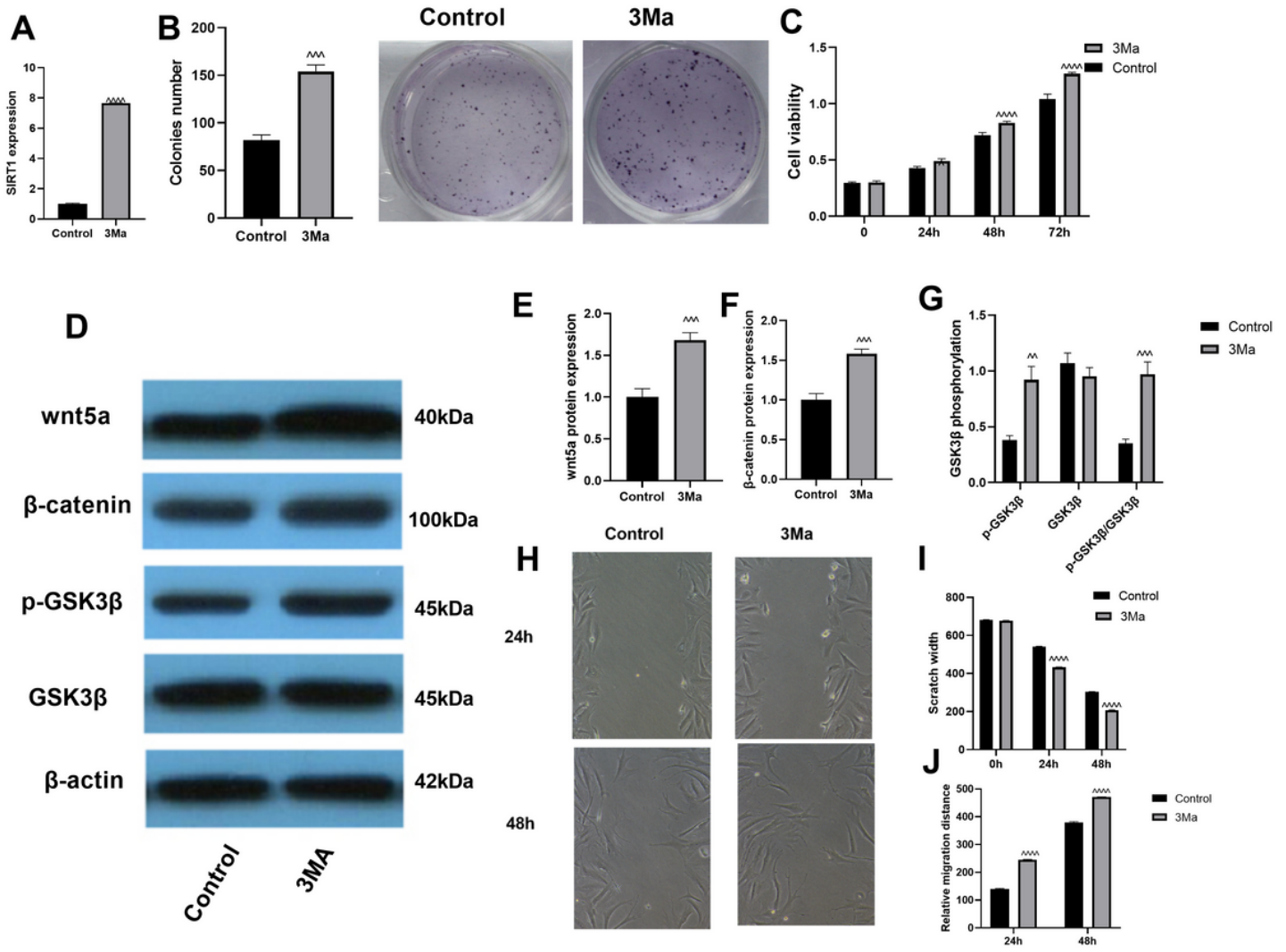

Figure 5

Autophagy inhibition led to the downregulation of SIRT1 expression in EPCs, attenuated cell proliferation and inactivated the wnt/β-catenin/GSK3β signaling pathway. EPCs in CAS group were cultured with the addition of autophagy inhibitor, 3Ma. A. RT-PCR evaluated the SIRT1 expression in cells in autophagy inhibition group in comparison with the CAS control group. B. colony formation methods were used to measure the proliferation of EPCs in CAS and 3Ma group. C. MTT method evaluated the cell viability. E-G. Western blot method detected the protein expression changes in the signaling pathway and the grey values were analyzed using Image J. H-J. Scratch medthods analyzed the migration ability. ****P<0.0001, ***P<0.001, **P<0.01, *P<0.05.

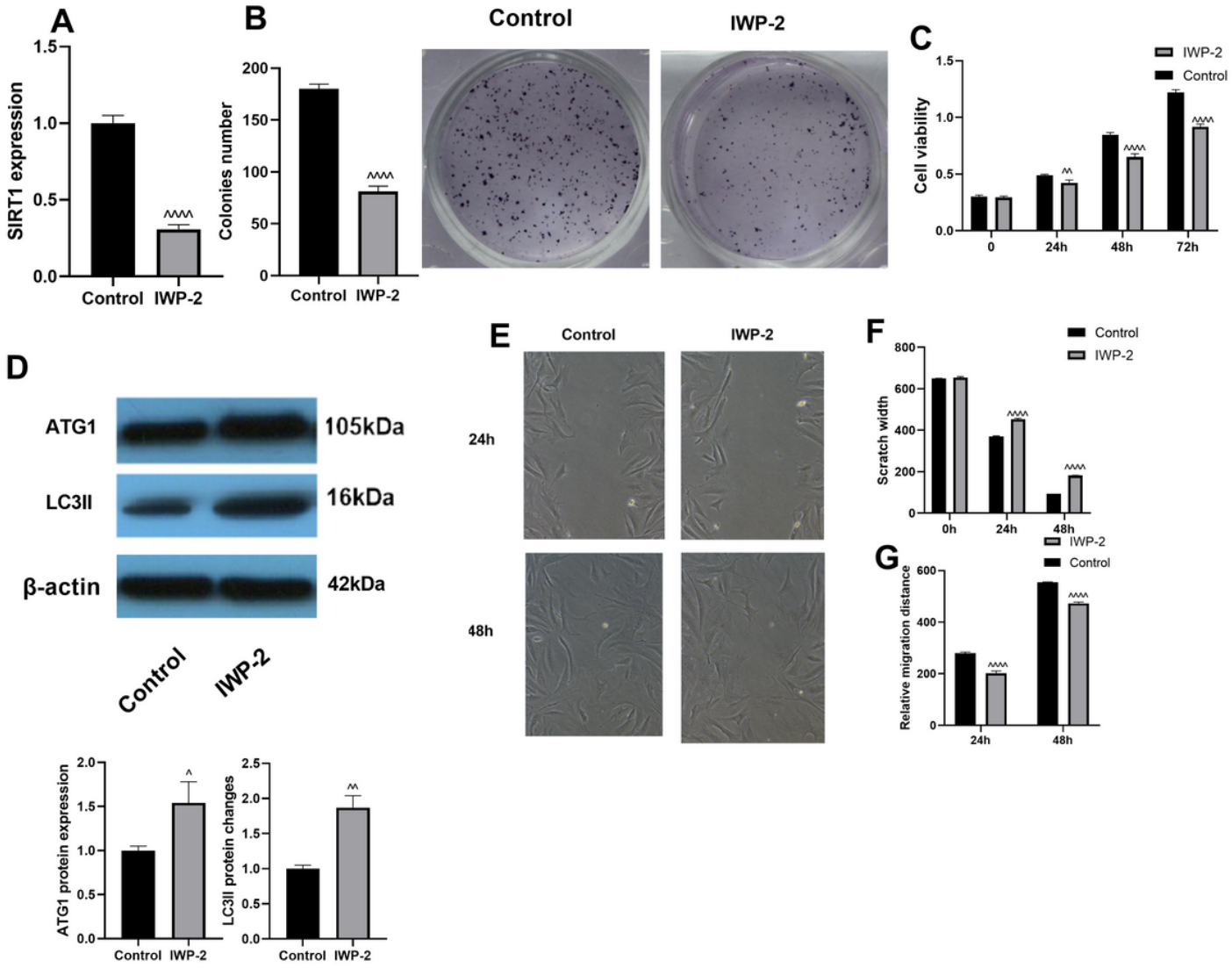

Figure 6

IWP-2 inhibited autophagy and proliferation of EPCs by inhibited the wnt/β-catenin/GSK3β signaling pathway The EPCs from the CAS group were selected for further treatment by wnt/β-catenin/GSK3β signaling inhibitor, IWP-2. A. RT-PCR measured SIRT1 mRNA expression with β-actin as internal control. B. Colony formation detected the EPC proliferation. C. MTT evaluated the cell viability. D-G. Western blot method detected the protein expression changes in autophagy-related genes and the grey values were analyzed using Image J. H-J. Scratch medthods analyzed the migration ability. ****P<0.0001, ***P<0.001, **P<0.01, *P<0.05.